

Gauged linear sigma model and pion-pion scattering

Amir H. Fariborz, ^{a *}, N.W. Park ^{b,c †}, Joseph Schechter ^{b §}, and M. Naeem Shahid ^{b ¶}

^b *Department of Physics, Syracuse University, Syracuse, NY 13244-1130, USA,*

^a *Department of Mathematics/ Science, State University of New York,
Institute of Technology, Utica, NY13504-3050, USA, and*

^c *Department of Physics, Chonnam National University, Gwangju, 500-757, South Korea,*

(Dated: November 5, 2018)

A simple gauged linear sigma model with several parameters to take the symmetry breaking and the mass differences between the vector meson and the axial vector meson into account is considered here as a possibly useful “template” for the role of a light scalar in QCD as well as for (at a different scale) an effective Higgs sector for some recently proposed walking technicolor models. An analytic procedure is first developed for relating the Lagrangian parameters to four well established (in the QCD application) experimental inputs. One simple equation distinguishes three different cases: i. QCD with axial vector particle heavier than vector particle, ii. possible technicolor model with vector particle heavier than the axial vector one, iii. the unphysical QCD case where both the KSRF and Weinberg relations hold. The model is applied to the s-wave pion-pion scattering in QCD. Both the near threshold region and (with an assumed unitarization) the “global” region up to about 800 MeV are considered. It is noted that there is a little tension between the choice of “bare” sigma mass parameter for describing these two regions. If a reasonable “global” fit is made, there is some loss of precision in the near threshold region.

PACS numbers: 14.80.Bn, 11.30.Rd, 12.39.Fe

I. INTRODUCTION

The linear sigma model [1] containing the pion field and a scalar field, sigma has played a very important role in particle physics during the last half century. Originally, it helped to clarify the role of chiral symmetry and its spontaneous breakdown [2] in strong interaction physics. The partial conservation of the axial currents together with their algebraic structure resulted in calculations for low energy pion physics which gave, for the first time, reasonable agreements with experiment. While the original calculations [3] were roundabout, it was found that they could be greatly simplified by straightforward perturbative calculations in the non-linear version of the model obtained by assuming the sigma field to be very heavy. Experimental evidence at that time did not clearly demand a light sigma meson.

Remarkably, the original linear version also turned out to be useful at a higher energy scale as the Higgs potential [4] of the electroweak standard model, with the sigma identified as the Higgs field.

More recently there has been some renewal of interest in the linear model for two different reasons. First, many people began to accept that a light sigma plays an important, but slightly hidden, role in low energy pion scattering. Second, the idea of “walking technicolor” theories [5] has gained some popularity. These theories furnish interesting candidates for an *effective* Higgs sector which has some similarity to the effective chiral Lagrangians associated with the color QCD theory. Such effective Lagrangians usually include, in addition to spin 0 fields, spin 1 fields since “vector meson dominance” is a well established feature of low energy strong interactions. Especially, the interplay of the composite technicolor vector and axial vector bosons appears to play an important role.

Our initial motivation is the further understanding of the properties of light scalar mesons. This is essentially connected with the s-wave pion pion scattering problem and also with the generalization to three light flavors of the underlying quarks. Some characteristic papers in the recent revival of interest in this subject are [6]-[33]. A fascinating aspect is the possibility that the light scalars contain two quarks and two antiquarks rather than one quark and one antiquark [31]. Consideration of the surprisingly light masses of such a “four quark” scalar nonet together with the surprisingly heavy candidates for a different, conventional “two quark” nonet suggests [35] a mixing between the two nonets. As discussed in section V of [36], it seems instructive to formulate this in a chiral invariant

* Email: fariboa@sunyit.edu

† Email: nwpark@jnu.ac.kr

§ Email: sachte@phy.syr.edu

¶ Email: mnshahid@phy.syr.edu

way using a generalized SU(3) linear sigma model. This enables one to formally distinguish four quark vs two quark mesons by means of their differing axial U(1) transformations as well as to compare four quark contents of scalar and pseudoscalar states. Other related work on mixing includes [37]- [42]. Now in these generalized sigma models there are more than one scalar and the s-wave scattering is more complicated. At least qualitatively, the s-channel is dominated by these scalars. In the region near threshold, the lowest mass sigma is most important. Thus, as a start to studying the effects of the vector mesons in such models, it seems natural to go back to the original linear sigma model and add the vector meson, rho with its chiral partner. Of course, this is not a new subject. A review of older work is given in [43] and recent papers include those in [44] .

Even though the plain linear sigma model is quite simple to deal with, the addition of spin 1 fields increases the overall complexity by an order of magnitude. In this paper the vector and axial vector fields are added as (initially) Yang Mills gauge fields. The local gauge symmetry is then manifestly broken by the addition of the three simplest chiral invariant spin 1 field mass terms. A somewhat new feature of the present work is that the determination of all Lagrangian parameters is carried out analytically with respect to the experimental inputs. The s-wave pion scattering is studied both for the threshold region and for the region away from threshold which is expected to be influenced by the presence of the lightest sigma. The scattering is explicitly compared with that of the plain linear sigma model as well as with experiment.

Because we have a simple connection between the Lagrangian parameters and the physical inputs, it is straightforward for us to also discuss application of the model to the non-QCD, but presumably chiral, situation which describes the walking technicolor theories. In particular, the case [45] where the vector meson is heavier than the axial vector meson will be treated in detail.

In section II, we expand the model Lagrangian in terms of the component fields representing the scalar σ , the pseudoscalar, $\vec{\pi}$ the vector \vec{V}_μ and the axial vector, \vec{A}_μ . Section III first discusses the diagonalization necessitated by the $\vec{A}_\mu \cdot \partial_\mu \vec{\pi}$ term in the Lagrangian. This results in “physical” pion and axial vector fields denoted with tildes. In general, the tilde will also be used on other objects to denote the fact that they are “physical”. Especially, in this section, the crucial job of determining the parameters of the Lagrangian from experiment will be discussed in detail. In section IV the complicated formula for the invariant Mandelstam amplitude in pion-pion scattering is computed at tree level. The s-wave partial wave amplitudes with I=0 and I=2 are then given explicitly. Section V discusses these amplitudes near threshold and also briefly explains their unitarizations by the K-matrix method. In section VI, the behaviors of the s-wave amplitudes away from threshold are treated. Section VII discusses some connections of this model with some interesting other work; first the limit of the present model in which the Weinberg [46] and Kawarabayashi Suzuki Riazuddin Fayazuddin (KSFR) [47] relations both hold is discussed. In addition, a systematic treatment of the model is given for the case in which (going beyond the application to low energy QCD) the vector meson mass is greater than the axial vector meson mass. Section VIII provides additional discussion. In the Appendix, it is explicitly shown how the scattering amplitude reproduces the “current algebra” result of the chiral model without spin 1 fields in the limit where the sigma mass goes to infinity.

II. LAGRANGIAN

Here, we present the version of the $SU_L(2) \times SU_R(2)$ gauged linear sigma model Lagrangian to be studied. The basic fields are the scalar, σ and pion, $\vec{\pi}$, which are contained in $M = (\sigma + i\vec{\pi} \cdot \vec{\tau})/\sqrt{2}$ and its Hermitian conjugate. The starting piece is the kinetic term for M , which is invariant under the chiral transformation, $M' = U_L M U_R^{-1}$. One can naturally introduce the left (l_μ) and the right (r_μ) vector fields by gauging the chiral symmetry. The resulting gauge invariant Lagrangian density is then,

$$\mathcal{L} = -\frac{1}{2}Tr(F_{\mu\nu}^r F_{\mu\nu}^r + F_{\mu\nu}^l F_{\mu\nu}^l) - \frac{1}{2}Tr(D_\mu M^\dagger D_\mu M), \quad (1)$$

where the covariant derivatives of M and M^\dagger are,

$$\begin{aligned} D_\mu M &= \partial_\mu M - igl_\mu M + igMr_\mu, \\ D_\mu M^\dagger &= \partial_\mu M^\dagger - igr_\mu M^\dagger + igM^\dagger l_\mu, \end{aligned} \quad (2)$$

and the field strength tensors take the form,

$$\begin{aligned} F_{\mu\nu}^l &= \partial_\mu l_\nu - \partial_\nu l_\mu - ig[l_\mu, l_\nu], \\ F_{\mu\nu}^r &= \partial_\mu r_\nu - \partial_\nu r_\mu - ig[r_\mu, r_\nu]. \end{aligned} \quad (3)$$

The vector and axial vector mesons are defined as

$$\begin{aligned} V_\mu &= l_\mu + r_\mu = \frac{1}{\sqrt{2}} \vec{V}_\mu \cdot \vec{\tau}, \\ A_\mu &= l_\mu - r_\mu = \frac{1}{\sqrt{2}} \vec{A}_\mu \cdot \vec{\tau}. \end{aligned} \quad (4)$$

The terms which contribute to particle masses are:

$$-m_0^2 \text{Tr}(l_\mu l_\mu + r_\mu r_\mu) + B \text{Tr}(M r_\mu M^\dagger l_\mu) - C \text{Tr}(l_\mu^2 M M^\dagger + r_\mu^2 M^\dagger M) - V_0(M, M^\dagger) - V_{SB}. \quad (5)$$

The first, m_0^2 term, which breaks the gauge invariance (and also the formal scale symmetry), gives the same mass to the vector and the axial vector mesons. The C term also gives the same mass to both spin 1 mesons, but maintains the scale symmetry. The B term breaks the mass degeneracy of the two spin 1 mesons. This is important since, experimentally, the lightest isovector, axial vector meson with negative G-parity (the $a_1(1260)$ is heavier than the rho meson. Another contribution to this mass splitting arises from spontaneous chiral symmetry breaking in the model, but this effect by itself will be seen to be insufficient. The last two terms are the scalar potential terms which respectively yield the spontaneous chiral symmetry breaking and the explicit symmetry breaking due to the small quark mass; explicitly,

$$V_0(M, M^\dagger) = a_1(\sigma^2 + \vec{\pi} \cdot \vec{\pi}) + a_3(\sigma^2 + \vec{\pi} \cdot \vec{\pi})^2, \quad V_{SB} = -2\sqrt{2}A\sigma. \quad (6)$$

Here, a_3 is positive while a_1 is chosen to be negative so that spontaneous chiral symmetry breaking will give a nontrivial vacuum expectation value v for σ . The explicit symmetry breaking term V_{SB} mocks up the light quark mass terms. The coefficients in this potential can be determined by the minimum condition in terms of the sigma and pion mass parameters, with the definition $V \equiv V_0 + V_{SB}$, as follows:

$$\begin{aligned} \left\langle \frac{\partial V}{\partial \sigma} \right\rangle = 0 &= 2a_1 v + 4a_3 v^3 - 2\sqrt{2}A, \\ \left\langle \frac{\partial^2 V_0}{\partial \sigma^2} \right\rangle = m_\sigma^2 &= 2a_1 + 12a_3 v^2, \\ \left\langle \frac{\partial^2 V_0}{\partial \pi^2} \right\rangle = m_\pi^2 &= 2a_1 + 4a_3 v^2. \end{aligned} \quad (7)$$

From this, one can easily derive the coefficients,

$$\begin{aligned} m_\pi^2 &= \frac{2\sqrt{2}A}{v}, \\ a_1 &= \frac{1}{2}(m_\sigma^2 - \frac{3}{2}(m_\sigma^2 - m_\pi^2)), \\ a_3 &= \frac{m_\sigma^2 - m_\pi^2}{8v^2}. \end{aligned} \quad (8)$$

The potential terms can be expressed in terms of the fields as:

$$\begin{aligned} V_0(M, M^\dagger) &= \frac{1}{2}m_\pi^2 \vec{\pi} \cdot \vec{\pi} + \frac{1}{2}m_\sigma^2 \sigma^2 + \frac{1}{2}g_{\sigma\pi\pi} \sigma \vec{\pi} \cdot \vec{\pi} + \frac{1}{4}g_4 (\vec{\pi} \cdot \vec{\pi})^2 + \dots, \\ g_{\sigma\pi\pi} &= \frac{m_\sigma^2 - m_\pi^2}{v}, \quad g_4 = \frac{2g_{\sigma\pi\pi}}{v}. \end{aligned} \quad (9)$$

Here, quadrilinear terms involving σ have not been written. Also note that the quantities m_π , $g_{\sigma\pi\pi}$ and g_4 are not the physical ones, which will be defined later.

Now, we express the rest of the Lagrangian in terms of the component fields. The spin zero meson kinetic terms are:

$$\begin{aligned}
-\frac{1}{2}Tr(D_\mu M D_\mu M^\dagger) &= -\frac{1}{2}\partial_\mu \vec{\pi} \cdot \partial_\mu \vec{\pi} - \frac{1}{2}\partial_\mu \sigma \partial_\mu \sigma + \frac{g}{\sqrt{2}}\vec{A}_\mu \cdot (\sigma \overleftrightarrow{\partial}_\mu \vec{\pi}) - \frac{g}{2\sqrt{2}}\epsilon_{abc}V_{\mu a}(\pi_b \overleftrightarrow{\partial}_\mu \pi_c) \\
&+ g^2[-\frac{\sigma^2}{4}\vec{A}_\mu \cdot \vec{A}_\mu + \frac{1}{2}\epsilon_{abc}\sigma\pi_a V_{\mu b}A_{\mu c} + \frac{1}{4}(\vec{\pi} \cdot \vec{V}_\mu)^2 - \frac{1}{4}(\vec{\pi} \cdot \vec{\pi})(\vec{V}_\mu \cdot \vec{V}_\mu) - \frac{1}{4}(\vec{\pi} \cdot \vec{A}_\mu)^2].
\end{aligned} \tag{10}$$

Here, it is understood that $\sigma = v + \tilde{\sigma}$ where $\tilde{\sigma}$ is the physical σ field.
The Yang-Mills terms are:

$$\begin{aligned}
-\frac{1}{2}Tr(F_{\mu\nu}^r F_{\mu\nu}^r + F_{\mu\nu}^l F_{\mu\nu}^l) &= -\frac{1}{4}[(\partial_\mu V_{\nu a} - \partial_\nu V_{\mu a})^2 + (\partial_\mu A_{\nu a} - \partial_\nu A_{\mu a})^2] \\
&- \frac{g}{2\sqrt{2}}\epsilon_{abc}[(\partial_\mu V_{\nu c} - \partial_\nu V_{\mu c})(V_{\mu a}V_{\nu b} + A_{\mu a}A_{\nu b}) \\
&- (\partial_\mu A_{\nu c} - \partial_\nu A_{\mu c})(V_{\mu a}A_{\nu b} + A_{\mu a}V_{\nu b})] \\
&- \frac{g^2}{8}[(\vec{V}_\mu \cdot \vec{V}_\mu)^2 - (\vec{V}_\mu \cdot \vec{V}_\nu)^2 + (\vec{A}_\mu \cdot \vec{A}_\mu)^2 - (\vec{A}_\mu \cdot \vec{A}_\nu)^2 \\
&+ 2(\vec{V}_\mu \cdot \vec{V}_\nu)(\vec{A}_\mu \cdot \vec{A}_\nu) - 2(\vec{V}_\mu \cdot \vec{V}_\nu)(\vec{A}_\mu \cdot \vec{A}_\nu) \\
&+ 4(\vec{V}_\mu \cdot \vec{A}_\mu)(\vec{V}_\nu \cdot \vec{A}_\nu) - 2(\vec{V}_\mu \cdot \vec{A}_\nu)(\vec{V}_\nu \cdot \vec{A}_\mu)].
\end{aligned} \tag{11}$$

Finally, the spin one meson mass terms are:

$$\begin{aligned}
-m_0^2 Tr(l_\mu l_\mu + r_\mu r_\mu) &= -\frac{1}{2}m_0^2(\vec{V}_\mu \cdot \vec{V}_\mu + \vec{A}_\mu \cdot \vec{A}_\mu), \\
-CTr(l_\mu^2 M M^\dagger + r_\mu^2 M^\dagger M) &= -\frac{C}{4}(\vec{V}_\mu \cdot \vec{V}_\mu + \vec{A}_\mu \cdot \vec{A}_\mu)(\sigma^2 + \vec{\pi} \cdot \vec{\pi}), \\
BTr(M r_\mu M^\dagger l_\mu) &= B[\frac{1}{8}\sigma^2(\vec{V}_\mu \cdot \vec{V}_\mu - \vec{A}_\mu \cdot \vec{A}_\mu) - \frac{1}{2}\epsilon_{abc}\sigma\pi_a V_{\mu b}A_{\mu c} + \frac{1}{4}(\vec{\pi} \cdot \vec{V}_\mu)^2 \\
&- \frac{1}{8}(\vec{\pi} \cdot \vec{\pi})(\vec{V}_\mu \cdot \vec{V}_\mu) - \frac{1}{4}(\vec{\pi} \cdot \vec{A}_\mu)^2 + \frac{1}{8}(\vec{\pi} \cdot \vec{\pi})(\vec{A}_\mu \cdot \vec{A}_\mu)].
\end{aligned} \tag{12}$$

III. DIAGONALIZATION AND DETERMINATION OF PARAMETERS

In this model, we have the five parameters g , v , m_0^2 , B and C to be determined from experiment. g and v are intrinsic parameters of the model while m_0^2 , B and C represent different ways to introduce vector and axial vector masses. Specifically the vector and axial vector masses are given by:

$$\begin{aligned}
m_V^2 &= m_0^2 - \frac{Bv^2}{4} + C\frac{v^2}{2}, \\
m_A^2 &= m_0^2 + \frac{Bv^2}{4} + C\frac{v^2}{2} + \frac{g^2v^2}{2} \equiv m_0'^2 + \frac{g^2v^2}{2}.
\end{aligned} \tag{13}$$

We see, from the third term on the right hand side of Eq.(10), that the Lagrangian yields a pion-axial vector meson mixing term proportional to $v\vec{A}_\mu \cdot \partial_\mu \vec{\pi}$. The Lagrangian can be diagonalized by introducing the physical (tilde) quantities as

$$\begin{aligned}
\vec{A}_\mu &= \tilde{A}_\mu + b\partial_\mu \tilde{\pi}, \\
\vec{\pi} &= w\tilde{\pi}.
\end{aligned} \tag{14}$$

b is determined from the condition of zero mixing between the physical pion and the physical axial vector meson, while w is determined from the condition of correct normalization of the pion kinetic term. We find

$$\begin{aligned}
b &= \frac{gv}{\sqrt{2}wm_0'^2}, \\
w &= \sqrt{1 + \frac{g^2v^2}{2m_0'^2}}.
\end{aligned} \tag{15}$$

The following alternate forms also are useful:

$$b = \frac{gvw}{\sqrt{2}m_A^2}$$

$$w^2 = \frac{m_A^2}{m_0^2} = \frac{1}{1 - \frac{g^2v^2}{2m_A^2}} \quad (16)$$

Note that m_0^2 was defined in Eq.(13) above. The physical pion decay constant, \tilde{F}_π is obtained from the Noether's theorem calculation of the single particle contributions to the axial current in our Lagrangian:

$$(J_\mu^A)_1^2 = -\sqrt{2}v \left(\frac{\partial L}{\partial(\partial_\mu\pi)} \right)_1^2 = \partial_\mu \left(\frac{\vec{\tau} \cdot \vec{\pi}}{\sqrt{2}} \right)_1^2 - \frac{gv}{\sqrt{2}} \left(\frac{\vec{\tau} \cdot \vec{A}_\mu}{\sqrt{2}} \right)_1^2$$

$$= \frac{\sqrt{2}v}{w} \partial_\mu \tilde{\pi}^+ - gv^2 \tilde{A}_\mu^+, \quad (17)$$

where we used Eq.(14) and, for example, $\tilde{\pi}^+$ is the physical positive pion field.

The coefficient in front of $\partial_\mu \tilde{\pi}^+$ is identified as the physical pion decay constant:

$$\tilde{F}_\pi = \frac{\sqrt{2}v}{w}. \quad (18)$$

Finally, we determine the $\rho\pi\pi$ interaction terms. For this purpose we collect the terms of this type from Eqs.(10) and (11) wherein the pion- axial vector diagonalization given in Eq.(14) is taken into account:

$$\mathcal{L}_{\rho\pi\pi} = \epsilon_{abc} V_{\mu a} \tilde{\pi}_b \partial_\mu \tilde{\pi}_c \left[-\frac{g}{\sqrt{2}} w^2 + \frac{wg^2bv}{2} + \frac{wBbv}{2} \right] - \frac{gb^2}{\sqrt{2}} \epsilon_{abc} \partial_\mu V_{\nu c} \partial_\mu \tilde{\pi}_a \partial_\nu \tilde{\pi}_b. \quad (19)$$

The last term constitutes a three derivative piece of the $\rho\pi\pi$ interaction. Note that, if one wishes to express it as an effective single derivative interaction, there will be a different result for $\rho \rightarrow \pi\pi$ decay (where ρ is on mass shell) and π - π scattering (where ρ is off mass shell).

From this, we can obtain the effective $\rho\pi\pi$ coupling constant for on-shell rho as:

$$g_{\rho\pi\pi}^{eff} = g \left(1 - \frac{Bv^2}{2m_0^2} - \frac{b^2}{2} m_\rho^2 \right). \quad (20)$$

The coupling constant $g_{\rho\pi\pi}^{eff}$ is related to the ρ meson width by

$$\Gamma(\rho) = (g_{\rho\pi\pi}^{eff})^2 |q_\pi|^3 / (12\pi m_\rho^2). \quad (21)$$

For $\Gamma(\rho) = 149.4$ MeV, one finds $|g_{\rho\pi\pi}^{eff}| \approx 8.66$.

Now we will solve for the vacuum value, v by the following procedure. First replace w in the second of Eqs.(15) by, from Eq.(18), the quantity $\sqrt{2}v/\tilde{F}_\pi$. Then replace $2m_0^2$ by, using Eqs.(13), $2m_A^2 - g^2v^2$. Squaring both sides gives the quadratic equation for v^2 :

$$v^4 - \frac{2m_A^2}{g^2} v^2 + \frac{2m_A^2 \tilde{F}_\pi^2}{2g^2} = 0. \quad (22)$$

This can be solved easily in terms of g^2v^2 to get:

$$g^2v^2 = m_A^2 \left(1 \pm \sqrt{1 - \frac{g^2 \tilde{F}_\pi^2}{m_A^2}} \right). \quad (23)$$

This is an equation which determines the product gv in terms of g and experimentally known quantities. We can find another relation between g and v by substituting $Bv^2/2 = m_A^2 - m_\rho^2 - g^2v^2/2$ and $b = gv w / (\sqrt{2}m_A^2)$ into Eq.(20):

$$g_{\rho\pi\pi}^{eff} = g \left(1 - \frac{1}{2m_A^2 - g^2v^2} \left(2(m_A^2 - m_\rho^2) - g^2v^2 \left(1 - \frac{m_\rho^2}{2m_A^2} \right) \right) \right) \quad (24)$$

Substituting Eq.(23) into Eq.(24) gives an equation for the Yang-Mills coupling constant, g by itself. Knowing this we can substitute back into Eq.(23) to determine v . Then we can determine B from:

$$B = \frac{2}{v^2}(m_A^2 - m_\rho^2) - g^2. \quad (25)$$

Finally, we may determine the linear combination, $m_0^2 + Cv^2/2$ from:

$$m_0^2 + Cv^2/2 = (m_\rho^2 + m_A^2)/2 - g^2v^2/4. \quad (26)$$

Note that from the four given inputs it is only possible to obtain the given linear combination of m_0^2 and C . Later we will consider two different ‘‘models’’ corresponding to either $m_0 = 0$ or $m_0 \neq 0$. Table I shows the results based on the best fit value of m_A as well as its maximum and minimum values. Note also that the solution requires the sign in Eq.(23) to be positive. The solutions with zero value for the square root and with the minus sign will be discussed in a later section.

m_A in GeV	g	v in GeV	w	b in GeV^{-1}	B	$m_0^2 + Cv^2/2$ in GeV^2
1.270	7.83	0.2	2.2	1.55	-12.9	0.456
1.230	7.78	0.197	2.13	1.53	-13.73	0.467
1.190	7.72	0.19	2.06	1.51	-14.65	0.468

TABLE I: $g, v, w, b, B, m_0^2 + Cv^2/2$ as functions of the axial vector meson mass. We used $\tilde{F}_\pi = 0.131$ GeV, $m_\rho = 0.775$ GeV, $g_{\rho\pi\pi}^{eff} = 8.56$ as inputs. Note that g, w and B are dimensionless.

It can be seen that the predicted parameters are not much affected by the uncertainty in the mass of the $a_1(1260)$ meson. Thus we will use the central value in what follows.

IV. PION-PION SCATTERING AMPLITUDE

At tree level, the conventional Mandelstam scattering amplitude, $A(s, t, u)$ has the following contributions:

1) Zero derivative contact term:

$$\begin{aligned} & -\tilde{g}_{\sigma\pi\pi}w^2/v, \\ \tilde{g}_{\sigma\pi\pi} & \equiv \frac{w^2}{v}(m_\sigma^2 - \frac{\tilde{m}_\pi^2}{w^2}). \end{aligned} \quad (27)$$

Note that Eqs.(9) and (14) were used in obtaining this result.

2) Two derivative contact term:

$$\left(\frac{g^2}{2} + B - C\right)b^2w^2s - Bb^2\tilde{m}_\pi^2w^2 + 2b^2C\tilde{m}_\pi^2w^2. \quad (28)$$

Note that the factor b^2 is due to the presence of a physical pion field in the original axial vector meson field, A_μ , as described in the first of Eqs.(14). Thus, b^2 labels the two derivative interaction terms.

3) Four derivative contact term:

$$-\frac{g^2}{2}b^4(2s^2 - t^2 - u^2 - 12\tilde{m}_\pi^2s + 16\tilde{m}_\pi^4) \quad (29)$$

Note, as above, that the b^4 factor indicates these terms arise from the quartic Yang-Mills interaction of the axial vector gauge field.

4) Sigma pole in the s- channel:

$$\frac{1}{m_\sigma^2 - s}[-\tilde{g}_{\sigma\pi\pi} + \sqrt{2}\tilde{m}_\pi^2gbw - 2G(\tilde{m}_\pi^2 - \frac{s}{2})]^2, \quad (30)$$

where,

$$G = -\frac{vg^2b^2}{2} - \frac{vBb^2}{4} + \frac{2gbw}{\sqrt{2}} - \frac{C}{2}b^2v. \quad (31)$$

5) Rho poles in the t and u channels:

$$\frac{s-u}{m_\rho^2-t}[-G_1 + \frac{gb^2}{2\sqrt{2}}t]^2 + \frac{s-t}{m_\rho^2-u}[-G_1 + \frac{gb^2}{2\sqrt{2}}u]^2, \quad (32)$$

where,

$$G_1 = \frac{g}{\sqrt{2}}(1 - \frac{Bv^2}{2m_0'^2}). \quad (33)$$

The full amplitude $A(s,t,u)$ is, of course, the sum of all five pieces just written. Since it is rather complicated, we verify in the Appendix, that in the m_σ goes to infinity limit $A(s,t,u)$ reduces to the correct "current algebra form. Here, we will be interested in the $I = 0, 2$ projections:

$$\begin{aligned} T^0 &= 3A(s, t, u) + A(t, u, s) + A(u, s, t), \\ T^2 &= A(t, u, s) + A(u, s, t), \end{aligned} \quad (34)$$

where the Mandelstam variables are $s = 4(p_\pi^2 + \tilde{m}_\pi^2)$, $t = -2p_\pi^2(1 - \cos\theta)$, $u = -2p_\pi^2(1 + \cos\theta)$, p_π being the spatial momentum of the pion in the center of mass frame.

The angular momentum l partial wave elastic scattering amplitude for isospin I is then defined as,

$$T_l^I = \frac{1}{64\pi} \sqrt{1 - \frac{4\tilde{m}_\pi^2}{s}} \int_{-1}^1 d\cos\theta P_l(\cos\theta) T^I(s, t, u). \quad (35)$$

Using the above formula, we get:

$$\begin{aligned} T_0^0 &= \frac{1}{64\pi} \sqrt{1 - \frac{4\tilde{m}_\pi^2}{s}} \left[10 \left(\frac{m_\sigma^2 - \tilde{m}_\pi^2/w^2}{v^2} w^4 + (2C - B)b^2 w^2 \tilde{m}_\pi^2 \right) + \frac{6}{m_\sigma^2 - s} [-\tilde{g}_{\sigma\pi\pi} + \sqrt{2}\tilde{m}_\pi^2 gbw - 2G(\tilde{m}_\pi^2 - \frac{s}{2})]^2 \right. \\ &\quad + 2(C_1^2 S_1 + 2C_1 G S_2 + G^2 S_3) + 4(G_1^2 R_1 + G_1 \frac{gb^2}{\sqrt{2}} R_2 + \frac{g^2 b^4}{8} R_3) - \frac{3g^2 b^4}{8} (4s^2 - \frac{64p_\pi^4}{3} - 24\tilde{m}_\pi^2 s + 32\tilde{m}_\pi^4) \\ &\quad \left. - \frac{g^2 b^4}{4} (-2s^2 + \frac{32p_\pi^4}{3} + 48\tilde{m}_\pi^2 s + 32\tilde{m}_\pi^4) + 6b^2 w^2 (\frac{g^2}{2} + B - C)s + 2b^2 w^2 (\frac{g^2}{2} + B - C)(-4p_\pi^2) \right] \end{aligned} \quad (36)$$

where

$$\begin{aligned} C_1 &= -\tilde{g}_{\sigma\pi\pi} + \sqrt{2}\tilde{m}_\pi^2 gbw - 2G\tilde{m}_\pi^2, \\ S_1 &= \frac{1}{2p_\pi^2} \ln(\frac{m_\sigma^2 + 4p_\pi^2}{m_\sigma^2}), S_2 = m_\sigma^2 S_1 - 2, S_3 = 4p_\pi^2 + m_\sigma^2 S_2, \\ R_1 &= \frac{1}{2p_\pi^2} \ln(\frac{m_\rho^2 + 4p_\pi^2}{m_\rho^2})(s + m_\rho^2 + 4p_\pi^2) - 2, R_2 = m_\rho^2 R_1 - 4p_\pi^2 - 2s, R_3 = m_\rho^2 R_2 + \frac{16p_\pi^4}{3} + 4p_\pi^2 s. \end{aligned} \quad (37)$$

Similarly for the $I = 2$ case:

$$\begin{aligned} T_0^2 &= \frac{1}{64\pi} \sqrt{1 - \frac{4\tilde{m}_\pi^2}{s}} \left[4 \left(\frac{m_\sigma^2 - \tilde{m}_\pi^2/w^2}{v^2} w^4 + (2C - B)b^2 w^2 \tilde{m}_\pi^2 \right) \right. \\ &\quad - 4(C_1^2 S_1 + 2C_1 G S_2 + G^2 S_3) + 4(G_1^2 R_1 + 2G_1 gb R_2 + gb^2 R_3) \\ &\quad \left. - \frac{g^2 b^4}{4} (-2s^2 + \frac{32p_\pi^4}{3} + 48\tilde{m}_\pi^2 s + 32\tilde{m}_\pi^4) + 2b^2 w^2 (\frac{g^2}{2} + B - C)(-4p_\pi^2) \right] \end{aligned} \quad (38)$$

V. SCATTERING NEAR THRESHOLD

Using the well known experimental results for the rho mass and width as well as the $a_1(1260)$ mass, we specified in Table I the Lagrangian parameters g , v , w , b , B and the linear combination $m_0^2 + Cv^2/2$. The only remaining "unknowns" are the "bare" mass of the sigma, m_σ and the relative sizes of m_0^2 and C . For definiteness we will

initially consider the case, $m_0 = 0$; soon we will see that the case, $m_0 \neq 0$, gives a poorer fit in the region away from threshold. Then the near threshold scattering will depend just on the value, m_σ . Of course one first considers the s-wave scattering lengths.

The scattering length $m_\pi a_0^0$ is plotted in Fig. 1 as a function of m_σ . Also shown are the predictions in the case of the “pure” linear sigma model, in which the vector and axial vector mesons are absent. It is seen that any given value of $m_\pi a_0^0$ (above the “current algebra” value of about 0.16 [48]) may be obtained for some m_σ . However, for a given value of the scattering length, m_σ is seen to be substantially lower when the vector and axial vector mesons are present. The experimental value of about 0.22 is obtained for $m_\sigma \approx 550$ MeV in the plain linear sigma model but for $m_\sigma \approx 360$ MeV in the model containing the spin 1 mesons. Fig.2 similarly shows the dependence of the non-resonant scattering length, $m_\pi a_0^2$ on m_σ .

Note that, for example,

$$\tilde{m}_\pi a_0^0 = \frac{T_0^0}{\rho}, \quad \rho = \sqrt{1 - 4\tilde{m}_\pi^2/s}, \quad (39)$$

wherein T_0^0/ρ is evaluated at threshold, remembering to first cancel the overall factor of ρ in T_0^0 . The amplitude is purely real in the present tree approximation. It is clearly convenient to compare with the real part of the partial wave amplitude. The experimental real part, R_0^0 is related to the experimental phase shift, δ_0^0 as

$$R_0^0 = \frac{1}{2} \sin(2\delta_0^0). \quad (40)$$

In Fig.3, for orientation, some values of R_0^0 near threshold obtained from the phase shifts found by the Na48/2 experiment [49] are shown. It can be seen that these data points near threshold may be reasonably explained by a value of $m_\sigma \approx 0.42$ GeV in the present model including spin 1 mesons but with the larger value $m_\sigma \approx 0.62$ GeV in the model without spin 1 mesons. It is hard to distinguish the two fits at the lower energies but above $\sqrt{s} \approx 0.35$ MeV the two model curves begin to diverge from each other and also to approach the unitarity bound, $R_0^0 = 1/2$. Clearly, the accuracy of the model must be improved to obtain a “global” description of the physics which does not violate the unitarity bound.

An easy way to cure this theoretical problem in the present model is to use the well known K matrix unitarization. As applied to Eq.(36), we identify the “Born” term T_0^0 with K and write for the unitarized partial wave amplitude, $(T_0^0)_U$:

$$(T_0^0)_U = \frac{T_0^0}{1 - iT_0^0}. \quad (41)$$

Clearly, near threshold, where T_0^0 is small, the unitarized amplitude is essentially the same as the non-unitarized one. This unitarization is actually familiar in ordinary scattering since it converts a generic simple pole into a Breit Wigner form. Diagrammatically, it has the structure of a “bubble sum”. It is easy to verify [50] that the scattering length is unchanged from the value obtained at tree level with this type of unitarization. Although the amplitude is now exactly unitary, it is important to recognize that this K-matrix procedure is, after all, a model.

VI. SCATTERING AWAY FROM THRESHOLD

Fig. 4 shows the unitarized amplitudes, just defined, calculated up to 1 GeV. Both the linear model with $m_\sigma = 0.62$ GeV and the present model with additional spin 1 fields and $m_\sigma = 0.42$ GeV are again seen to start the same way. However afterwards, the spin 1 model amplitude rises more sharply and has its first zero, as required [since $R_0^0 \equiv T_0^0/(1 + (T_0^0)^2)$ goes to zero when T_0^0 goes to infinity] at 0.42 GeV while the plain linear model amplitude has its first zero at 0.62 GeV. The shapes of these two curves do not fit the experimental data beyond the threshold region very well. A more realistic fit would correspond, for example, to a plain linear sigma model which has its first zero in the 0.85 GeV region; see Fig. 8 and Table II in the first paper in ref. [36]. (It is also seen there that the addition of the scalar $f_0(980)$ in that SU(3) linear sigma model framework allows one to fit the peculiar looking amplitude from about 0.8 GeV to about 1.2 GeV.) As a check of the validity of this “global” fit up to about 0.8 GeV we note that the sigma pole position came out to be in decent agreement with the one recently obtained by a detailed analysis [51] of the experimental data. The sigma pole position in the complex s plane is found by separating the tree amplitude, Eq.(36) into pole and non-pole pieces as:

$$T_0^0 = \alpha(s) + \frac{\beta(s)}{m_\sigma^2 - s}. \quad (42)$$

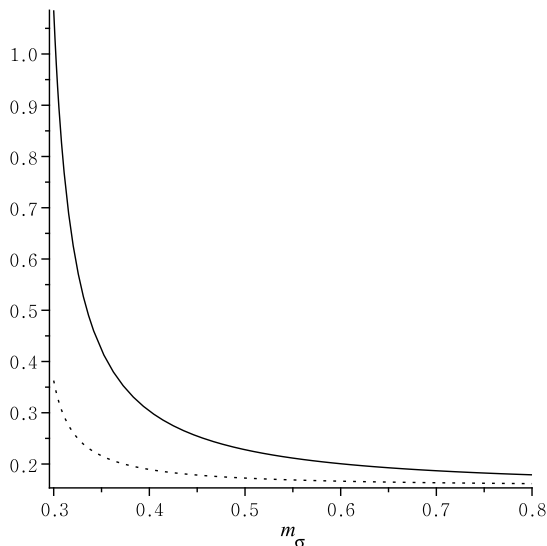


FIG. 1: The scattering length $m_\pi a_0^0$ as a function of the sigma mass in GeV. The solid line: pure linear sigma model. The dotted line: the present model including spin 1 mesons.

Then the pole position, z in the complex s plane for the K-matrix unitarized amplitude, $(T_0^0)_U$ is the solution to the equation,

$$(m_\sigma^2 - z)(1 - i\alpha(z)) - i\beta(z) = 0. \quad (43)$$

We find the numerical result in the simple K-matrix unitarized linear sigma model without spin 1 particles, $z^{1/2} = 0.51 - i0.23$. This may be compared with the recent value, $z^{1/2} = 0.461 - i0.255$, with an uncertainty of about .015 in each term. In Fig. 5 the model amplitudes for both the plain linear sigma model and the one with spin 1 particles are plotted up to 1.4 GeV using $m_\sigma = 0.85$ GeV just mentioned. The case including spin 1 particles was calculated with the choice $m_0^2 = 0$ so that $C \neq 0$. (Remember that only the combination $m_0^2 + Cv^2/2$ is known from our inputs.) While, as we just mentioned, the curve for the plain linear sigma model essentially fits the data, the curve representing the model with spin 1 particles is a rather rough approximation to it. This can be verified by noting that the pole position comes out to be, $z^{1/2} = 0.38 - i0.52$. The fit is not improved by lowering the value of m_σ .

It is also of some interest to look at the dependence of the predicted amplitude on the parameter m_0^2 . for the case with spin 1 particles. The results for the non-zero choice, $m_0^2 = 0.27$ GeV² are shown in Fig. 6. In this case the predictions for the $m_0^2 \neq 0$ case seem to be further distorted, showing that $m_0^2 = 0$ provides a better fit.

How much does the $m_\sigma = 0.85$ GeV choice, which was used for the region up to about 0.8 GeV change the fit to the data close to threshold obtained with smaller values of m_σ ? This is shown in Fig. 7. Clearly, both plots lie below the low energy data. Thus there is some tension between a reasonable fit close to threshold (which requires a low value of m_σ) and a fit over a larger range (which requires a larger value of m_σ).

Of course, it is clear that the direct channel $f_0(980MeV)$ state must be also included to adequately treat the scalar I=0 amplitude in the region from 800 to about 1200 MeV. We consider this region to be beyond the range of applicability of the model with a single sigma state.

VII. CONNECTIONS WITH OTHER WORK

In the historical treatment of chiral models containing vector and axial vector mesons as well as the pion, two plausible relations among their parameters - the KSRF [47] and Weinberg [46] formulas have been widely discussed. Eventually, it was accepted that they are not forced to hold by chiral symmetry but in some limit can be correlated with each other. These formulas are, respectively,

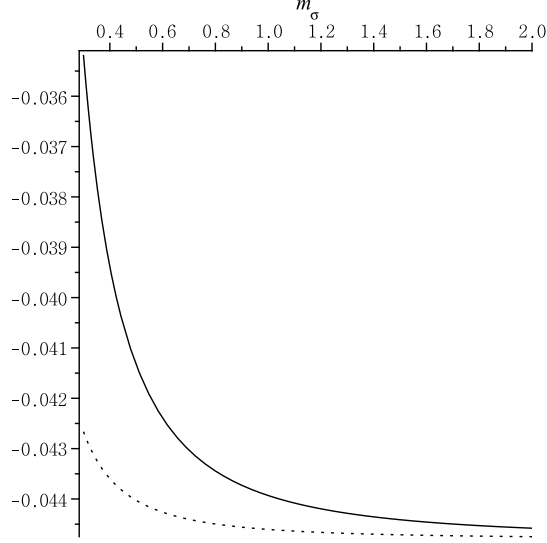


FIG. 2: The scattering length $m_\pi a_2^0$ as a function of the sigma mass in GeV. The solid line: pure linear sigma model. The dotted line: present model including spin 1 mesons.

$$\begin{aligned} (g_{\rho\pi\pi}^{eff})^2 &= 2m_\rho^2/\tilde{F}_\pi^2, \\ m_A^2 &= 2m_\rho^2. \end{aligned} \quad (44)$$

Numerically, the first relation holds to about 4 percent while the second only holds to about 26 percent.

In the present work it was not necessary to use either of these formulas. Nevertheless, it may be interesting to first briefly discuss the limit of our model which correlates the two formulas. This limit corresponds to, first, approximating $g_{\rho\pi\pi}^{eff}$ by g and, second, setting $B=0$. We will show that the Weinberg relation then implies the KSRF relation. From both of Eqs.(13) we then note that w^2 in Eq.(16) becomes simply,

$$w^2 = \frac{m_A^2}{m_\rho^2} = 2. \quad (45)$$

Eq.(18) then reads $v^2 = \tilde{F}_\pi^2$ so that,

$$m_A^2 - m_\rho^2 = m_\rho^2 = g^2 v^2 / 2 = g^2 \tilde{F}_\pi^2 / 2, \quad (46)$$

which is the KSRF relation. Note that approximating $g_{\rho\pi\pi}^{eff}$ by g amounts physically to neglecting the B term in the Lagrangian as well as the induced three derivative $\rho\pi\pi$ interaction term. It is also seen that the two equations in Eq.(44) hold at the special point where the square root in Eq.(23) vanishes (with $B=0$).

An interesting different possible application of the present chiral model containing vector and axial vector mesons is to the effective Higgs sector of the minimal walking technicolor theory [5]. That theory may provide the mechanism for constructing a technicolor model which gives consistent values of the electroweak ‘‘oblique’’ parameters. A characteristic feature is the situation where the vector boson is heavier than the axial vector boson. To investigate this possibility we now search for more general parameter solutions, including those with the negative sign in Eq.(23).

It is convenient to define

$$\chi = \frac{g^2 v^2}{2m_A^2}. \quad (47)$$

Then the pion wave function renormalization is given by,

$$w^2 = \frac{1}{1 - \chi}. \quad (48)$$

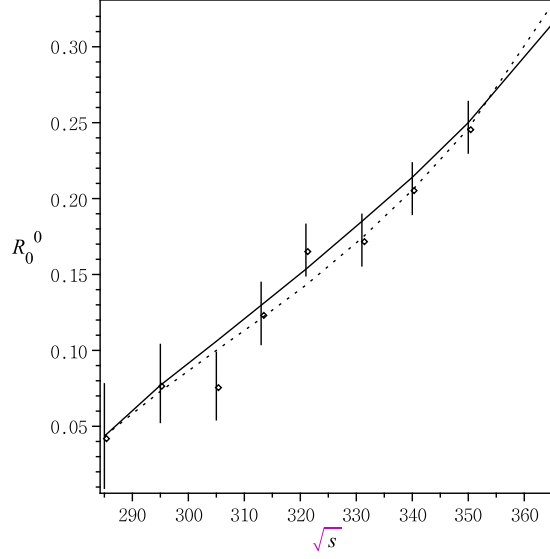


FIG. 3: Low energy data for real part of s-wave resonant amplitude plotted against \sqrt{s} in MeV. The dotted curve is a fit to the present model with $m_\sigma = 0.42$ GeV while the solid curve is a fit to the plain linear sigma model with $m_\sigma = 0.62$ GeV

Eq.(23) then reads:

$$\chi = \frac{1}{2} \left(1 \pm \sqrt{1 - \frac{g^2 \tilde{F}_\pi^2}{m_A^2}} \right), \quad (49)$$

Notice that to have a consistent solution for the parameters we must require:

$$g^2 \leq m_A^2 / \tilde{F}_\pi^2. \quad (50)$$

Finally, Eq.(24) can be rewritten as,

$$g_{\rho\pi\pi}^{eff} = \frac{g\tau}{2} \left(\frac{2 - \chi}{1 - \chi} \right), \quad (51)$$

where we defined, for convenience,

$$\tau = \frac{m_\rho^2}{m_A^2}. \quad (52)$$

Note especially that when Eq.(49) is inserted into Eq.(51), we can use it to find $g_{\rho\pi\pi}^{eff}$ as a function of g for given values of the physical quantities, \tilde{F}_π and m_A . This determines g and then v etc.

In Fig.8, in which the plus sign in Eq.(49) has been chosen, the lower curve displays $g_{\rho\pi\pi}^{eff}$ as a function of g for the physical choice,

$$\tau_{QCD} = \left(\frac{m_\rho}{m_A} \right)^2 \approx 0.4. \quad (53)$$

We see that the physical value, $g_{\rho\pi\pi}^{eff} \approx 8.56$ corresponds to the value $g = 7.78$, which is safely below the bound at,

$$\frac{m_A}{\tilde{F}_\pi} = 9.46. \quad (54)$$

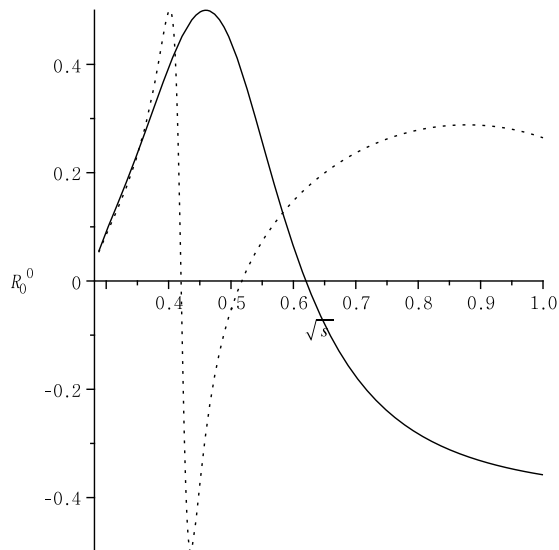


FIG. 4: Unitarized amplitudes plotted as a function of \sqrt{s} to 1 GeV. The dashed curve corresponds to the present model with $m_\sigma = 0.42$ GeV while the solid curve corresponds to the plain linear sigma model with $m_\sigma = 0.62$ GeV.

The upper curve in Fig.8 corresponds, for illustration of the $m_\rho > m_A$ case, to a choice, $\tau=1.2$. In this case we have no experimentally a priori way of specifying the physical parameters and the bound. Nevertheless, we observe that $g_{\rho\pi\pi}^{eff}$ would be exceptionally large for a reasonable solution.

In Fig.9, which corresponds to the choice of the minus sign in Eq.(49), it is seen that the QCD case (lower curve) has no consistent parameter solution since $g_{\rho\pi\pi}^{eff}=8.56$ can not be achieved for $g < 9.46$. On the other hand, the upper curve, which corresponds again to $\tau = 1.2$, gives reasonable values of $g_{\rho\pi\pi}^{eff}$.

To summarize: the QCD case corresponds to the plus sign choice in Eq.(49) while a possible consistent parameter solution in a non-QCD setting with $m_\rho > m_A$ is likely to correspond to the minus sign choice.

It is amusing to observe that the relation between the vacuum value v and \tilde{F}_π differs for the two sign choices:

$$\begin{aligned} \tilde{F}_\pi &< v && (+sign), \\ \tilde{F}_\pi &> v && (-sign). \end{aligned} \quad (55)$$

To see this note that for the plus sign case, Eq.(49) gives $1/2 < \chi < 1$ which, using Eq.(48) translates to $w > \sqrt{2}$ and the desired result when Eq.(18) is noted. The minus sign case is obtained similarly after first noting $1 < w < \sqrt{2}$ in that situation.

We have seen that the choice of sign in Eq.(49) distinguishes the two cases where m_ρ is less than or greater than m_A . This choice occurs in fitting the parameters to experiment. It may be of some interest to ask how this distinction is related to the parameters of the effective Lagrangian directly. To investigate this, we just subtract the second of Eqs.(13) from the first:

$$m_\rho^2 - m_A^2 = -\frac{v^2}{2}(B + g^2). \quad (56)$$

In the QCD case, Table I shows that B is negative and that the right hand side above is negative because $g^2 > |B|$. In the case which should correspond to a walking technicolor theory we evidently must require, if B is also negative, the opposite condition $g^2 < |B|$. That condition seems intuitively plausible. Since B is the coefficient of a scale invariant term in the effective Lagrangian, we might expect it not to change sign in going from one theory to the other. Furthermore, we would expect the phenomenological coupling constant g to behave something like the underlying gauge theory coupling constant and hence to decrease in strength for a “walking” theory [52].

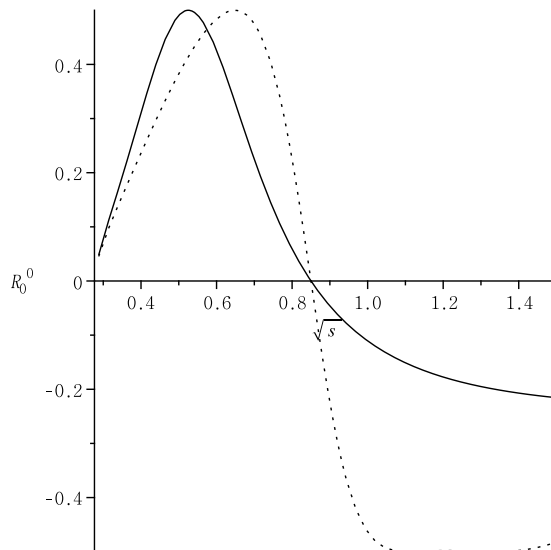


FIG. 5: Unitarized scattering amplitudes to 1.4 GeV with m_σ chosen to be 0.85 GeV for both the plain (solid curve) and spin 1 meson (dashed curve) sigma models. Here $m_0^2 = 0$ was assumed.

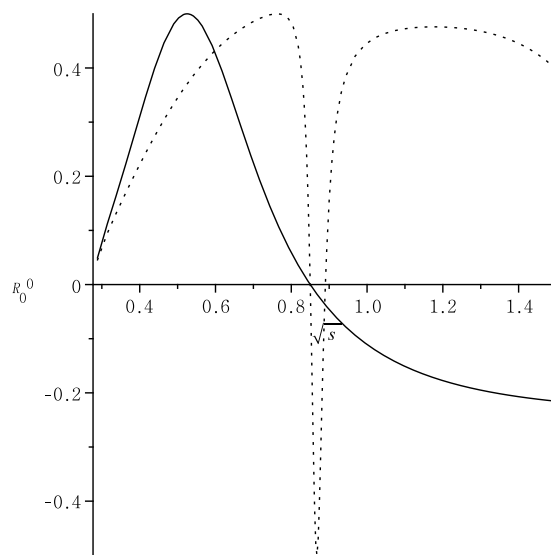


FIG. 6: Same as Fig. 5 but assuming $m_0^2 = 0.27 \text{ GeV}^2$ instead

VIII. SUMMARY AND FURTHER DISCUSSION

First, we argued that a detailed treatment of the gauged minimal linear sigma model would be very helpful for developing a better understanding of the light scalar mesons in QCD.

One quickly realizes, however, that such a model is much more complicated than the ungauged version. Hence, attention was first paid to developing an “analytic procedure” for relating the Lagrangian parameters to the four well

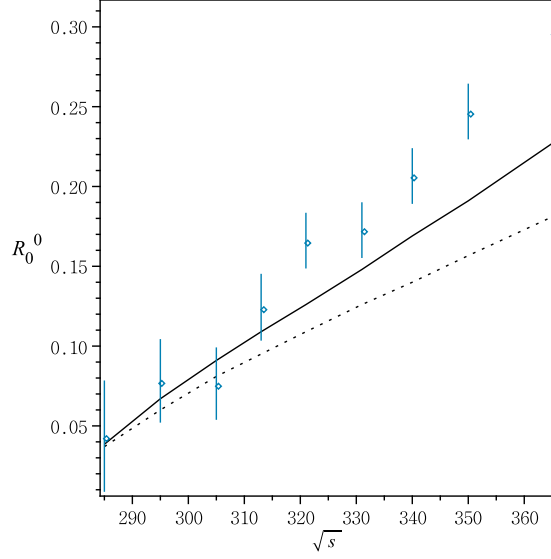


FIG. 7: Predictions for the choice $m_\sigma = 0.85$ GeV in the region near threshold. Same conventions as in Fig. 3

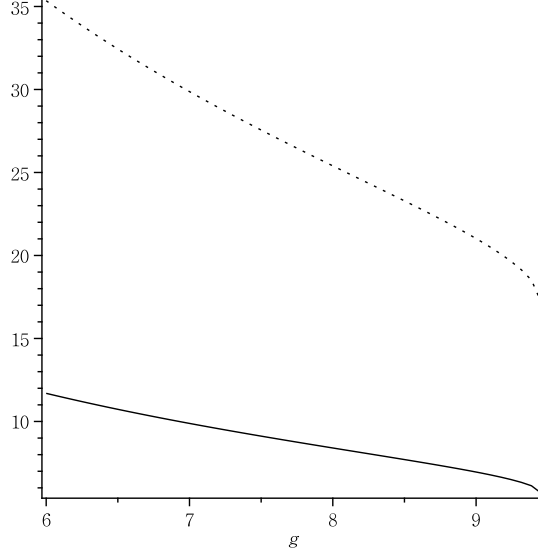


FIG. 8: $g_{\rho\pi\pi}^{eff}$ vs g with the plus sign in Eq.(49). The lower curve is the QCD case while the upper curve corresponds to a hypothetical "walking technicolor" case with $m_\rho > m_A$.

established experimental inputs: \tilde{F}_π , m_ρ , Γ_ρ and $m[a_1(1260)]$. The key equation obtained is Eq.(23) or equivalently, Eq.(49). If the minus sign in this equation is chosen, it was shown (in the last section) that there is no consistent solution of parameters when inputs are taken from the possible application to QCD of this model. On the other hand, the minus sign choice allows a solution with $m_\rho > m_A$, which is plausibly related to a "minimal walking technicolor" application of the effective Lagrangian. If the plus sign choice is made in this equation, it was shown that the QCD application of the model is allowed though a "walking technicolor" application, while possible, seems to correspond

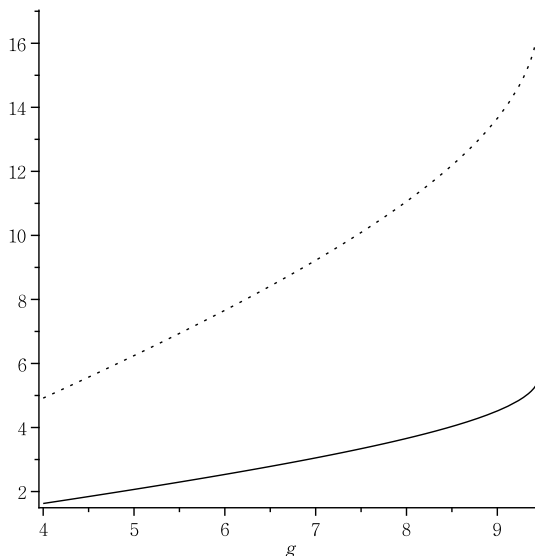


FIG. 9: $g_{\rho\pi\pi}^{eff}$ vs g with the minus sign in Eq.(49). The lower curve is the QCD case while the upper curve corresponds to a hypothetical "walking technicolor" case with $m_\rho > m_A$.

to an extremely large rho boson width. There is also a special case in this equation when the square root vanishes so the sign choice is irrelevant. In that situation, the Weinberg and KSRF relations are both satisfied in the unphysical limit where $B=0$.

In this work we did not impose either the Weinberg or KSRF relations. The model is self-contained and represents a spontaneously broken chiral $SU(2)$ symmetry with an assumed particle spectrum of pi, sigma, rho and $a_1(1260)$.

As a check, before comparing the computed s wave pion pion scattering to experiment, we verified (in the Appendix) that the complicated formula for the amplitude reduces to that of the non-linear sigma model without vectors when the sigma mass goes to infinity.

To begin the study of the scattering amplitude in the resonant s-wave channel we fit the near threshold NA48/2 data [49] up to about 370 MeV using the tree amplitude. A good fit was obtained by choosing the bare sigma mass, m_σ to be about 420 MeV. A similarly good fit in the sigma model without spin 1 fields needed m_σ to be about 620 MeV instead (See Fig. 3). Once a value of m_σ is chosen, the amplitude is also predicted at higher energies. It was pointed out (see Fig. 4 that those values of m_σ resulted in "global" pictures of the s-wave scattering which was considerably distorted. Much better "global" pictures emerge from choices of bare sigma mass, m_σ about 850 MeV. However such a value for m_σ results in, as seen in Fig. 7, some loss of precision for the region just near threshold. From the standpoint of learning about the sigma, the higher bare sigma mass is evidently the more suitable one.

The feature of getting similar fits with or without vectors, but with different values of the sigma parameters which emerged in the discussions in sections V and VI had been already observed some time ago [19]. In that case, the non-linear 3-flavor chiral Lagrangian was used instead and the region from threshold to about 1.2 GeV was fit. Rather than the K-matrix method, a phenomenological unitarization scheme was employed. It seems that the light sigma and the $f_0(980)$ are, not surprisingly, the main features of the $I=0$, s-wave pion-pion scattering amplitude in this energy range. Adding the rho meson changes somewhat the parameters of the sigma needed for fitting.

Comparing the "global" fits to the resonant s-wave pion pion scattering amplitude up to about 800 MeV, it is seen that the linear sigma model without the spin 1 particles actually gives a better fit than the one with the spin 1 particles included. This seems to be due to the higher polynomial terms induced by the Yang Mills interaction.

If one takes the present model at face value, the underlying Lagrangian appears to describe all the contained particles as quark anti-quark composites. In the mixing picture mentioned earlier [35]- [42], where all the particles are mixtures of these "2 quark" states with "4 quark" states, this work should be modified to include two different chiral multiplets and the 2-flavor case upgraded to the 3 flavor case for more realism. This has been done for the case without vectors and axial vectors in the mentioned references so adding the spin 1 particles in that framework is a next step. We would expect that the general behaviors of the lowest lying sigma and the rho and $a_1(1260)$ would be

similar to those in the present model.

Also in the application to the minimal walking technicolor model [5], the present piece would have to be embedded in a larger framework with an initial $SU(4)$ symmetry. One might similarly expect that the behaviors of the sigma (=Higgs) and the technicolor spin 1 bosons would be similar to those seen here [53].

Acknowledgments

We are happy to thank A. Abdel-Rehim, D. Black, M. Harada, R. Jora, S. Moussa, S. Nasri and F. Sannino for helpful related discussions. The work of A.H.F. has been partially supported by the NSF Grant 0652853. The work of N.W.P. is supported by Chonnam National University. The work of J.S. and M.N.S. is supported in part by the U. S. DOE under Contract no. DE-FG-02-85ER 40231.

APPENDIX A: LARGE SIGMA MASS LIMIT

We verify here that, in the large sigma mass limit, our scattering amplitude reproduces the well-known result of the chiral model: $A(s, t, u) = 2(s - \tilde{m}_\pi^2)/\tilde{F}_\pi^2$.

The most crucial piece is the sigma pole contribution in the s channel given by Eq.(30). We start by expanding the denominator:

$$\frac{1}{m_\sigma^2 - s} = \frac{1}{m_\sigma^2 - \tilde{m}_\pi^2/w^2} \left(1 + \frac{s - \tilde{m}_\pi^2/w^2}{m_\sigma^2 - \tilde{m}_\pi^2/w^2} + \mathcal{O}(1/m_\sigma^4)\right). \quad (\text{A1})$$

Next we rewrite the numerator of Eq.(30) so as to display the m_σ dependence:

$$\frac{w^4}{v^2}(m_\sigma^2 - \tilde{m}_\pi^2/w^2) + -2\frac{w^2}{v}(\sqrt{2}gbw\tilde{m}_\pi^2 - 2G(\tilde{m}_\pi^2 - \frac{s}{2})) + \dots, \quad (\text{A2})$$

where the dots indicate terms independent of m_σ^2 . These two equations give the result for Eq.(30):

$$\frac{w^4}{v^2}(m_\sigma^2 - \tilde{m}_\pi^2/w^2) + \frac{w^4}{v^2}(s - \tilde{m}_\pi^2/w^2) - 2\frac{w^2}{v}(\sqrt{2}gbw\tilde{m}_\pi^2 - 2G(\tilde{m}_\pi^2 - \frac{s}{2})). \quad (\text{A3})$$

Notice that the first term above is cancelled by Eq.(27). For simplicity we will consider the $C=0$ case since the C contribution ends up not contributing in the present limit. Then Eq.(28) just gives:

$$-Bb^2w^2\tilde{m}_\pi^2 + b^2w^2\left(B + \frac{g^2}{2}\right)s. \quad (\text{A4})$$

Next, note that the contribution of Eq.(29) is higher order in \tilde{m}_π^2 and hence negligible for the present purpose. Finally, the rho pole contribution of Eq.(32) to leading order has the form

$$G_1^2 \frac{3s - 4\tilde{m}_\pi^2}{m_\rho^2}. \quad (\text{A5})$$

The net result so far consists of Eq.(A3) without the first term, Eq.(A4) and Eq.(A5).

We use the following expressions to simplify these terms:

$$\begin{aligned} 2\sqrt{2}\frac{w^2}{v}gbw &= \frac{4}{v^2}w^2(w^2 - 1), \\ 4G\frac{w^2}{v} &= \frac{4}{v^2}(w^2 - 1)(w^2 + 1) - \frac{2B}{g^2v^2}(w^2 - 1)^2, \\ G_1^2 &= \frac{g^2}{2}\left(1 - \frac{Bv^2}{2m_0^2}\right)^2, \\ b^2w^2 &= \frac{2}{g^2v^2}(w^2 - 1)^2. \end{aligned} \quad (\text{A6})$$

Then, the part of $A(s, t, u)$ proportional to s is:

$$s\left[\frac{1}{v^2}((3-2w^2) + \frac{3B}{g^2}(w^2-1)^2 + \frac{3g^2v^2}{2m_\rho^2}(1 - \frac{B}{g^2}(w^2-1))^2)\right], \quad (\text{A7})$$

while the part proportional to \tilde{m}_π^2 is:

$$\tilde{m}_\pi^2\left[-\frac{w^2}{v^2} - \frac{4}{v^2}w^2(w^2-1) + \frac{4}{v^2}(w^2-1)(w^2+1) - \frac{4B}{g^2v^2}(w^2-1)^2 - \frac{2g^2}{m_\rho^2}\left(1 - \frac{B}{g^2}(w^2-1)\right)^2\right]. \quad (\text{A8})$$

We will now show that Eq.(A7) is equal to $\frac{2s}{F_\pi^2}$. For this, we notice that the terms which do not include B in Eq.(A7) become

$$s\left[3 - 2w^2 + \frac{3g^2v^2}{2m_\rho^2}\right] = s\left[3 - 2w^2 + \frac{3}{2m_\rho^2}(2m_\rho^2 + Bv^2)(w^2 - 1)\right] = s\left[w^2 + \frac{3Bv^2}{2m_\rho^2}(w^2 - 1)\right], \quad (\text{A9})$$

where we used,

$$g^2v^2 = 2m_\rho'^2(w^2 - 1) = (2m_\rho^2 + Bv^2)(w^2 - 1). \quad (\text{A10})$$

Then, all B terms in Eq.(A7) and in Eq.(A9) can be arranged to give:

$$s\left[\frac{3B}{g^2}(w^2-1)\left(\frac{g^2v^2}{2m_\rho^2} - w^2 + 1 - \frac{Bv^2}{2m_\rho^2}(w^2-1)\right)\right]. \quad (\text{A11})$$

It is easily shown that this is equal to zero using the relation (A10). Then, we can see that Eq.(A7) becomes $\frac{sw^2}{v^2} = \frac{2s}{F_\pi^2}$, which is the desired result.

The \tilde{m}_π^2 part can be treated similarly. The terms which do not include B in Eq.(A8) become

$$\begin{aligned} \tilde{m}_\pi^2\left[-\frac{w^2}{v^2} - \frac{4}{v^2}w^2(w^2-1) + \frac{4}{v^2}(w^2-1)(w^2+1) - \frac{2g^2}{m_\rho^2}\right] \\ = \tilde{m}_\pi^2\left[-\frac{w^2}{v^2} - \frac{2B}{m_\rho^2}(w^2-1)\right]. \end{aligned} \quad (\text{A12})$$

The first term on the second line, $-\tilde{m}_\pi^2w^2/v^2$ is just $-2\tilde{m}_\pi^2/\tilde{F}_\pi^2$, while the second term is proportional to B. Then all terms linear in B in Eq.(A8) become

$$\begin{aligned} \tilde{m}_\pi^2\left[-\frac{2B}{m_\rho^2}(w^2-1) - \frac{4B}{g^2v^2}(w^2-1) + \frac{4B}{m_\rho^2}(w^2-1)\right] \\ = \tilde{m}_\pi^2\left[\frac{2B}{g^2v^2}(w^2-1)\left[2(w^2-1) - \frac{g^2v^2}{m_\rho^2}\right]\right] = \tilde{m}_\pi^2\left[\frac{2B^2}{g^2m_\rho^2}(w^2-1)^2\right], \end{aligned} \quad (\text{A13})$$

where in the second line, we used the relation, Eq.(A10). This term is exactly the negative of the B^2 term in Eq.(A8), so all B terms cancel out to give the desired result.

- [1] M. Gell-Mann and M. Levy, *Nuovo Cimento*, **16**, 705(1960). Here, we consider the version of this model where the nucleon fields are absent.
- [2] See also Y. Nambu and G. Jona-Lasinio, *Phys. Rev.* **122**, 345 (1961), **124**, 246 (1961).
- [3] S.L. Adler and R.F. Dashen, "Current Algebras and Application to Particle Physics", W.A. Benjamin, New York, 1968.
- [4] S. Weinberg, *Phys. Rev. Lett.* **19**, 1264 (1967); A. Salam, p. 367 of *Elementary Particle Theory*, ed. N. Svartholm (Almquist and Wiksells, Stockholm, 1969).

- [5] A detailed review of the "minimal walking technicolor" model is given in R. Foadi, M.T. Frandsen, T.A. Ryttev and F. Sannino, Phys. Rev. D **76**, 055005 (2007). See also F. Sannino, arXiv:0804.0182[hep-ph]. An historical review of the subject is given by K. Yamawaki, Proc. of the International Symposium pnA 50, PTP supplement no. 167, 127 (2007).
- [6] See the dedicated conference proceedings, S. Ishida et al "Possible existence of the sigma meson and its implication to hadron physics", KEK Proceedings 2000-4, Soryyushiron Kenkyu 102, No. 5, 2001. Additional points of view are expressed in the proceedings, D. Amelin and A.M. Zaitsev "Hadron Spectroscopy", Ninth International Conference on Hadron Spectroscopy, Protvino, Russia(2001) and A. H. Fariborz, "Scalar mesons, an interesting puzzle for QCD", Utica N. Y. (2003), AIP Conference Proceedings Vol. 688.
- [7] E. van Beveren, T.A. Rijken, K. Metzger, C. Dullemond, G. Rupp and J.E. Ribeiro, Z. Phys. **C30**, 615 (1986). E. van Beveren and G. Rupp, hep-ph/9806246, 248. See also J.J. de Swart, P.M.M. Maessen and T.A. Rijken, U.S./Japan Seminar on the YN Interaction, Maui, 1993 [Nijmegen report THEF-NYM 9403].
- [8] D. Morgan and M. Pennington, Phys. Rev. **D48**, 1185 (1993).
- [9] A.A. Bolokhov, A.N. Manashov, M.V. Polyakov and V.V. Vereshagin, Phys. Rev. **D48**, 3090 (1993). See also V.A. Andrianov and A.N. Manashov, Mod. Phys. Lett. **A8**, 2199 (1993). Extension of this string-like approach to the πK case has been made in V.V. Vereshagin, Phys. Rev. **D55**, 5349 (1997) and in A.V. Vereshagin and V.V. Vereshagin, *ibid.* **59**, 016002 (1999).
- [10] N.N. Achasov and G.N. Shestakov, Phys. Rev. **D49**, 5779 (1994).
- [11] R. Kaminski, L. Leśniak and J. P. Maillet, Phys. Rev. **D50**, 3145 (1994).
- [12] F. Sannino and J. Schechter, Phys. Rev. **D52**, 96 (1995).
- [13] N.A. Törnqvist, Z. Phys. **C68**, 647 (1995) and references therein. In addition see N.A. Törnqvist and M. Roos, Phys. Rev. Lett. **76**, 1575 (1996), N.A. Törnqvist, hep-ph/9711483 and Phys. Lett. **B426** 105 (1998).
- [14] R. Delbourgo and M.D. Scadron, Mod. Phys. Lett. **A10**, 251 (1995). See also D. Atkinson, M. Harada and A.I. Sanda, Phys. Rev. **D46**, 3884 (1992).
- [15] G. Janssen, B.C. Pearce, K. Holinde and J. Speth, Phys. Rev. **D52**, 2690 (1995).
- [16] M. Svec, Phys. Rev. **D53**, 2343 (1996).
- [17] S. Ishida, M.Y. Ishida, H. Takahashi, T. Ishida, K. Takamatsu and T Tsuru, Prog. Theor. Phys. **95**, 745 (1996), S. Ishida, M. Ishida, T. Ishida, K. Takamatsu and T. Tsuru, Prog. Theor. Phys. **98**, 621 (1997). See also M. Ishida and S. Ishida, Talk given at 7th International Conference on Hadron Spectroscopy (Hadron 97), Upton, NY, 25-30 Aug. 1997, hep-ph/9712231.
- [18] M. Harada, F. Sannino and J. Schechter, Phys. Rev. **D54**, 1991 (1996).
- [19] M. Harada, F. Sannino and J. Schechter, Phys. Rev. Lett. **78**, 1603 (1997).
- [20] D. Black, A.H. Fariborz, F. Sannino and J. Schechter, Phys. Rev. **D58**, 054012 (1998).
- [21] D. Black, A.H. Fariborz, F. Sannino and J. Schechter, Phys. Rev. **D59**, 074026 (1999).
- [22] J.A. Oller, E. Oset and J.R. Pelaez, Phys. Rev. Lett. **80**, 3452 (1998). See also K. Igi and K. Hikasa, Phys. Rev. **D59**, 034005 (1999).
- [23] A.V. Anisovich and A.V. Sarantsev, Phys. Lett. **B413**, 137 (1997).
- [24] V. Elias, A.H. Fariborz, Fang Shi and T.G. Steele, Nucl. Phys. **A633**, 279 (1998).
- [25] V. Dmitrasinović, Phys. Rev. **C53**, 1383 (1996).
- [26] P. Minkowski and W. Ochs, Eur. Phys. J. **C9**, 283 (1999).
- [27] S. Godfrey and J. Napolitano, hep-ph/9811410.
- [28] L. Burakovsky and T. Goldman, Phys. Rev. **D57** 2879 (1998)
- [29] T. Hatsuda, T. Kunihiro and H. Shimizu, Phys. Rev. Lett. **82**, 2840 (1999); S. Chiku and T. Hatsuda, Phys. Rev. D **58**, 076001 (1998).
- [30] L. Celenza, S-f Gao, B. Huang and C.M. Shakin, Phys. Rev. C **61**, 035201 (2000).
- [31] A diquark, anti-diquark nonet was explored in: R.L. Jaffe, Phys. Rev. D **15**, 267 (1977). A partial meson-meson nonet was advocated in: J.D. Weinstein and N. Isgur, Phys. Rev. Lett. **48**, 659 (1982) and also, Y. S. Kalashnikova, A. E. Kudryavtsev, A. V. Nefediev, C. Hanhart and J. Haidenbauer, Eur. Phys. J. A **24** (2005) 437.
- [32] The Roy equation for the pion amplitude, S.M. Roy, Phys. Lett. B **36**, 353 (1971), has been used by several authors to obtain information about the $f_0(600)$ resonance. See T. Sawada, page 67 of ref. [6] above, I. Caprini, G. Colangelo and H. Leutwyler, Phys. Rev. Lett. **96**, 132001 (2006). A similar approach has been employed to study the putative light kappa by S.Descotes-Genon and B. Moussallam, Eur. Phys. J. C **48**, 553 (2006).
- [33] Further discussion of the approach in ref. [32] above is given in D.V. Bugg, J. Phys. G **34**, 151 (2007) [hep-ph/0608081].
- [34] A. Zhang, T. Huang and T.G. Steele, hep-ph/0612146.
- [35] D. Black, A. H. Fariborz and J. Schechter, Phys. Rev. **D61** 074001 (2000).
- [36] D. Black, A.H. Fariborz, S. Moussa, S. Nasri and J. Schechter, Phys.Rev. **D64**, 014031 (2001). See also A.H. Fariborz, R. Jora and J. Schechter, Phys. Rev. D **77**, 094004 (2008) and E. Meggiolaro, Z. Phys. C **62**, 669 (1994).
- [37] T. Teshima, I. Kitamura and N. Morisita, J. Phys. G **28**, 1391 (2002); *ibid* **30**, 663 (2004); F. Close and N. Tornqvist, *ibid.* **28**, R249 (2002); A.H. Fariborz, Int. J. Mod. Phys. A **19**, 2095 (2004); 5417 (2004); Phys. Rev. D **74**, 054030 (2006); F. Giacosa, Th. Gutsche, V.E. Lyubovitskij and A. Faessler, Phys. Lett. B **622**, 277 (2005); J. Vijande, A. Valcarce, F. Fernandez and B. Silvestre-Brac, Phys. Rev. D **72**, 034025 (2005); S. Narison, Phys. Rev. D **73**, 114024 (2006); L. Maiani, F. Piccinini, A.D. Polosa and V. Riquer, hep-ph/0604018. J.R. Pelaez, Phys. Rev. Lett. **92**, 102001 (2004); J.R. Pelaez and G. Rios, Phys. Rev. Lett. **97**, 242002 (2006); F. Giacosa, Phys. Rev. D **75**,054007 (2007).
- [38] M. Napsuciale and S. Rodriguez, Phys. Rev. D **70**, 094043 (2004).
- [39] A.H. Fariborz, R. Jora and J. Schechter, Phys. Rev. D **72**, 034001 (2005); Phys. Rev. D **76**, 114001 (2007).
- [40] G. 't Hooft, G. Isidori, L. Maiani, A.D. Polosa and V. Riquer, Phys. Lett. B **662**, 424 (2008).

- [41] In K-F Liu, arXiv:0706.1262 [hep-ph], the author presents evidence from lattice theory for a picture of a scalar spectrum containing light four quark type states and heavier two quark type states.
- [42] In N. Yamamoto, M. Tachibana, T. Hatsuda and G. Baym, arXiv:0704.2654 [hep-ph] and A.A. Andrianov and D. Espriu, arXiv:0709.0049 [hep-ph] similar models are discussed for non zero temperature and pressure.
- [43] S. Gasiorowicz and D.A. Geffen, Rev. Mod. Phys. **41**, 531 (1968).
- [44] M.D. Scadron, F. Kleefeld and G. Rupp, arXiv:hep-ph/0601196; N. Achasov, arXiv:0810.2201[hep-ph]; S. Struber and D.H. Rischke, Phys. Rev. D **77**, 085004 (2008); D. Parganlija, F. Giacosa and D.H. Rischke, arXiv:0812.2183[hep-ph].
- [45] T. Applequist and F. Sannino, Phys. Rev. D **59**, 067702 (1999); R. Foadi, M.T. Frandsen, T.A. Rytto and F. Sannino, Phys. Rev. D **76**, 055005 (2007).
- [46] S. Weinberg, Phys. Rev. Lett. **18**, 507 (1967); T. Das, V. Mathur and S. Okubo, Phys. Rev. Lett. **18**, 761 (1967).
- [47] K. Kawarabayashi and M. Suzuki, Phys. Rev. Lett. **16**, 255 (1966); Riazuddin and Fayazuddin, Phys. Rev. **147**, 1071 (1966).
- [48] S. Weinberg, Phys. Rev. Lett. **17**, 616 (1966).
- [49] J.R. Batley et al [NA48/2 Collaboration], Eur. Phys. J. C **52**, 875 (2007)[arXiv:0707.0697]. See also R. Kaminski, J.R. Pelaez and F.J. Yndurian, Phys. Rev. D **77**, 054015 (2008).
- [50] See the discussion around Eq.(47) in the second reference of [39] given above.
- [51] R. Kaminski, R. Garcia-Martin, P. Gryniewicz and J.R. Pelaez, arXiv:0811.4510[hep-ph].
- [52] See for example Fig. 5 in the second paper in [5] above.
- [53] See also R. Foadi, M. Jarvinen and F. Sannino, arXiv:0811.3718[hep-ph].